Energy Provisioning and Operating Costs in Hybrid Solar Powered Infrastructure

Mohammad Sheikh Zefreh[1], Terence D. Todd[1] and George Karakostas[2]

[1]Department of Electrical and Computer Engineering
McMaster University
Hamilton, Ontario, CANADA
Email: todd@mcmaster.ca

[2]Department of Computing and Software
McMaster University
Hamilton, Ontario, CANADA
Email: karakos@mcmaster.ca

***Abstract*—In this paper we consider the operating and capital expenditure costs of solar powered additions to infrastructure that is operated from the power grid. The capital expenditure (CAPEX) costs are those associated with provisioning the solar power components, and are selected using an offline design optimization. Once the solar add-on is designed and deployed, the node incurs ongoing operating expenditure (OPEX) costs associated with the purchase of power grid energy. Lower bounds on cost are derived using a linear programming formulation, where the solar power components are sized using historical solar insolation traces and projected loading data. Different node add-on arrangements are considered, which result in various solar/battery and grid configurations. Three energy scheduling algorithms are then introduced to optimize online OPEX costs. A variety of results are presented that show the extent to which a solar powered add-on can reduce total cost. These results also show that the proposed algorithms give performance that is close to the lower bounds in many situations.**

I. Introduction

Solar power is commonly used in cases where power grid connections are unavailable or prohibitively expensive. In these systems, a major equipment cost is that of providing a suitable combination of solar panels and batteries so that the node can be operated without outage. The selection of solar components is referred to as "energy provisioning" and has been studied extensively in the past [1].

The energy provisioning cost of a solar powered node is a strong function it's average power consumption. For this reason, energy efficient designs will reduce both capital expenditure (CAPEX), and ongoing operational expenditure (OPEX) costs. For example, the goal of the Energy Aware Radio and Network Technologies (EARTH) project is to achieve a reduction in the energy consumption of mobile networks by 50% [2]. In [3], the design of a basestation that is powered by solar and diesel energy is analyzed, and in [4] a hybrid solar-wind powered basestation is described. A hybrid system consisting of solar, wind and diesel energy was designed in [5]. In these projects, the basestation use of solar and wind power is mainly in scenarios where there is no access to power grid connections. However, in [6] a hybrid configuration of grid and solar energy is considered. It is assumed that the cellular network consists of highly loaded BSs (HBS) that are powered by grid electricity, and solar powered BSs that are lightly loaded (LBS). An algorithm is proposed that minimizes the maximum energy depletion rates of the LBSs, therefore enabling more users to be served with green energy. The optimum number of green base stations in a cellular network is analyzed in [7].

The cost of solar components, will eventually decrease to the point where solar may be commonly used as an add-on for grid powered communications infrastructure. In this paper we consider a methodology that can be used to assess the costs of installing and operating a hybrid powered node solar add-on. The offline problem is formulated as a linear program (LP) which provides lower bounds on the OPEX and CAPEX costs. A variety of configurations are considered including conventional solar add-ons which give, solar panel/battery/grid, battery/grid, and panel/grid systems. These designs are compared on the basis of total CAPEX and OPEX costs. Three energy scheduling algorithms are introduced which operate on the online system and reduce the costs associated with power grid purchases. A variety of results are presented that show the conditions under which a solar powered add-on can reduce total cost. These results also show that the proposed algorithms give performance that is close to the lower bounds in many situations.

II. System Overview and Models

We consider a single outdoor communication node which provides some kind of fixed infrastructure functionality. It is assumed that the node is connected to the electrical power grid, but that the energy needed for continuous operation may be supplemented with a solar powered add-on as shown in Figure 1. The solar add-on includes solar panels that have been positioned to absorb the maximum possible solar energy, and an associated battery bank that can store both solar energy, and optionally, energy drawn from the power grid connection. The electrical inputs and outputs are interconnected through an *Energy Controller* which, among other things, provides protection from battery over and under-charging. There will also be an AC/DC converted block (not shown in the figure) between the power grid and the energy controller.

The total cost under consideration consists of the sum of Capital Expenditure (CAPEX) and Operating Expenditure (OPEX) costs over some defined time period. We assume that the node is already deployed with a power grid connection, and the CAPEX cost of interest is that associated with the provisioning of the solar power add-on to the existing system.

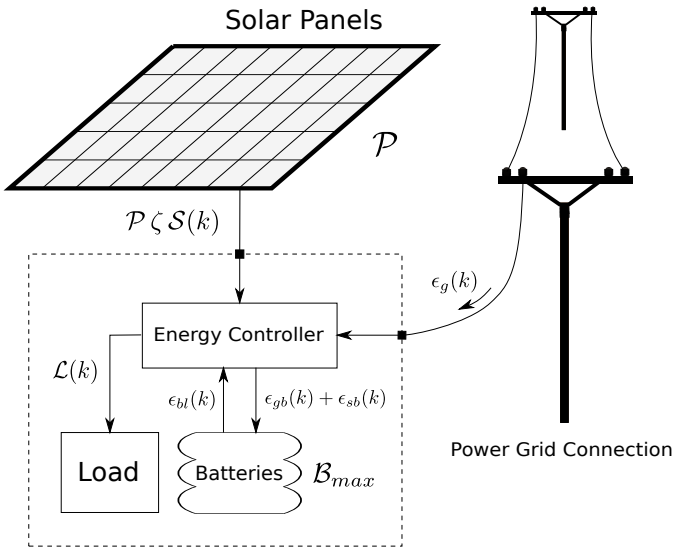

Fig. 1. Grid Powered Node with Solar Powered Add-on.

Battery Charge Efficiency, η_b^+	Panel-to-Grid Energy, $\epsilon_{sg}(\cdot)$
Battery Discharge Efficiency, η_b^-	Panel-to-Load Energy, $\epsilon_{sl}(\cdot)$
Residual Battery Energy, $\mathcal{B}(\cdot)$	Grid-to-Battery Energy, $\epsilon_{gb}(\cdot)$
Deployment Time, $\mathcal{T}$	Grid-to-Load Energy, $\epsilon_{gl}(\cdot)$
Battery Capacity, $\mathcal{B}_{max}$	Battery-to-Load Energy, $\epsilon_{bl}(\cdot)$
Minimum Battery Energy, $\mathcal{B}_{min}$	Harvested Energy, $\epsilon_s(\cdot)$
Solar Panel Size, $\mathcal{P}$	Energy Cost (/kWh), $c_g(\cdot)$
Panel Efficiency, ζ	Purchased Energy, $\epsilon_g(\cdot)$
Unit Battery Cost, c_b	Solar Energy Input, $\mathcal{S}(\cdot)$
Unit Panel Cost, c_p	Load Energy, $\mathcal{L}(\cdot)$
Panel-to-Battery Energy,$\epsilon_{sb}(\cdot)$	Energy Sale Price (/kWh), $r_g(\cdot)$

TABLE I
LIST OF PARAMETERS

Once the solar add-on is designed and installed, the solar energy used is "free" and does not contribute to on-going OPEX costs. For this reason, the major OPEX cost considered, is that of post-installation power grid electricity purchases. Our objective is to design the solar power add-on and control the energy flow so that the total costs are minimized over the time period considered.

Photo-voltaic modeling is normally done in discrete time, where the system is considered over some contiguous time period $\mathcal{T} \triangleq [0, K\Delta t]$, where K is a large integer. We define $\mathcal{K} = [1, 2, \ldots, K]$, where each $k \in \mathcal{K}$ corresponds to one Δt time epoch. It is also well accepted that for solar provisioning purposes, excellent accuracy may be obtained using $\Delta t = 1$ hour time increments [1]. For expository purposes, we consider the solar panel/battery/grid (PBG) configuration shown in Figure 1. We define $\mathcal{B}(k)$ as the residual energy in the battery at the end of time epoch k. Input energy flow to the battery during time period k consists of energy harvested from the solar panels, $\epsilon_{sb}(k)$, and energy purchased from the power grid, $\epsilon_{gb}(k)$. During the same time epoch, energy $\epsilon_{bl}(k)$ is drawn from the battery and consumed in the load. $\mathcal{B}_{min}$ and $\mathcal{B}_{max}$ are defined to be the minimum allowed battery level, and the battery capacity, respectively. Using these definitions, the energy in the battery at the end of time epoch k can be written as

$$\mathcal{B}(k) = \min\{\max\{\mathcal{B}(k-1) + \eta_b^+(\epsilon_{sb}(k) + \epsilon_{gb}(k)) - \epsilon_{bl}(k), \mathcal{B}_{min}\}, \mathcal{B}_{max}\} \quad \forall k \in \mathcal{K} \tag{1}$$

where η_b^+ is the charging efficiency of the battery. Equation (1) is a simple recursion that finds the battery energy at time k to be that at time $k-1$, plus the energy received from the solar panels and the power grid, minus the energy supplied from the battery to the load over that time period. Equation (1) uses the well known linear energy flow model that is commonly used for photovoltaic node energy provisioning [1]. In this model the load energy required during time epoch k is given by $\mathcal{L}(k)$. This can be supplied, directly from the solar panels without storage in the battery, from energy purchased from the power grid, and, from energy drawn from the battery. This gives the following load equation,

$$\mathcal{L}(k) = \epsilon_{sl}(k) + \epsilon_{gl}(k) + \eta_b^-\,\epsilon_{bl}(k) \quad \forall k \in \mathcal{K} \tag{2}$$

where $\epsilon_{sl}(k)$ and $\epsilon_{gl}(k)$ are the direct solar energy and power grid energy consumed in the load, and η_b^- is the battery discharge efficiency. Finally, the maximum energy that can be drawn from the battery in time epoch k must not exceed that which was available at the start of the interval, that is,

$$\epsilon_{bl}(k) \le \mathcal{B}(k-1) \quad \forall k \in \mathcal{K} \tag{3}$$

Assuming that $\epsilon_s(k)$ and $\epsilon_g(k)$ are the total harvested solar and purchased power grid energies in time epoch k, we must have that

$$\epsilon_s(k) = \epsilon_{sb}(k) + \epsilon_{sl}(k) \quad \forall k \in \mathcal{K} \tag{4}$$

$$\epsilon_g(k) = \epsilon_{gb}(k) + \epsilon_{gl}(k) \quad \forall k \in \mathcal{K}. \tag{5}$$

The term, $\epsilon_s(k)$, can be written as

$$\epsilon_s(k) = \mathcal{P}\,\zeta\,\mathcal{S}(k) \quad \forall k \in \mathcal{K} \tag{6}$$

where $\mathcal{P}$, ζ and $\mathcal{S}(k)$ are the solar panel size (i.e., area), efficiency, and the per unit area solar energy availability for an optimally oriented solar panel during time period k, respectively. Sample traces of historical values for $\mathcal{S}(k)$ which are used in this paper are available from meteorological databases. In the USA for example, this data is available from the U.S. Department of Energy [8]. The optimization parameters defined above are summarized in Table I.

III. HYBRID NODE TOTAL COST BOUNDS

Our objective is to minimize the total CAPEX and OPEX cost for the node over the time period $\mathcal{T}$. This can be found using the linear programs (LPs) formulated in this section. Different versions are given for various node configurations.

A. Solar Panel/Battery/Grid (PBG) Configuration

This is the basic configuration shown in Figure 1 which includes a solar panel and battery add-on. The inputs to the problem are given by the set of n-tuples

$$\mathcal{I} = \{(c_b, c_p, c_c, c_g(k), \mathcal{L}(k), \epsilon_s(k), \eta_b^+, \eta_b^-\} \quad \forall k \in \mathcal{K} \tag{7}$$

where c_p and c_b are the per unit solar panel and battery prices, respectively, and $c_g(k)$ is the power grid energy purchase price during time epoch k. Cost c_c is a cost which is included to accommodate other capital costs which may be incurred. For example, when considering the sale of energy to the power grid, c_c is used to model the added equipment costs needed to support this functionality. The LP finds a lower bound on the minimum total CAPEX and OPEX costs over the set of optimization variables defined by the n-tuples

$$\mathcal{V} = \{(\mathcal{B}_{max}, \mathcal{P}, \epsilon_g(k), \epsilon_{gb}(k), \epsilon_{gl}(k), \epsilon_{sb}(k), \epsilon_{sl}(k))\} \quad (8)$$

where $k \in \mathcal{K}$. The optimization, referred to as LP–PBG, is first given, and then described below.

$$\min_{\mathcal{V}} c_b\ \mathcal{B}_{max} + c_p\ \mathcal{P} + c_c + \sum_{k\in\mathcal{K}} c_g(k)\ \epsilon_g(k) \qquad \text{(LP–PBG)}$$

subject to

$$\begin{aligned}
&\mathcal{B}(k) \le \mathcal{B}(k-1) + \\
&\quad \eta_b^+(\epsilon_{sb}(k) + \epsilon_{gb}(k)) - \epsilon_{bl}(k) && \forall k \in \mathcal{K} && (9)\\
&\mathcal{L}(k) \le \epsilon_{sl}(k) + \epsilon_{gl}(k) + \eta_b^-\ \epsilon_{bl}(k) && \forall k \in \mathcal{K} && (10)\\
&\epsilon_{sb}(k) + \epsilon_{sl}(k) \le \epsilon_s(k) && \forall k \in \mathcal{K} && (11)\\
&\epsilon_{gb}(k) + \epsilon_{gl}(k) \le \epsilon_g(k) && \forall k \in \mathcal{K} && (12)\\
&\epsilon_{bl}(k) \le \mathcal{B}(k-1) && \forall k \in \mathcal{K} && (13)\\
&\mathcal{B}_{min} \le \mathcal{B}(k) && \forall k \in \mathcal{K} && (14)\\
&\mathcal{B}(k) \le \mathcal{B}_{max} && \forall k \in \mathcal{K} && (15)\\
&\epsilon_s(k) = \mathcal{P}\ \zeta\ \mathcal{S}(k) && \forall k \in \mathcal{K} && (16)\\
&\mathcal{B}(0) = \mathcal{B}_{max} && && (17)\\
&0 \le \epsilon_g(k), \epsilon_s(k), \epsilon_{gl}(k), \epsilon_{gb}(k) && \forall k \in \mathcal{K} && (18)\\
&0 \le \epsilon_{sl}(k), \epsilon_{sb}(k), \epsilon_{bl}(k), \mathcal{P}, \mathcal{B} && \forall k \in \mathcal{K} && (19)
\end{aligned}$$

The first two terms in the objective consist of the solar panel and battery CAPEX costs, and the third term is the sum of the OPEX costs of power grid purchases over $\mathcal{T}$. Inequality (9) expresses Equation (1) as an inequality constraint, as does (10) for Equation (2). Inequality (11) ensures that the solar energy stored and expended in the load during interval k cannot exceed that provided by the solar panel. Similarly, inequality (12) performs the same function for purchased power grid energy. Constraints (13) to (19) are the same that those discussed in results (3) to (6), plus the obvious non-negativity constraints on the energy and panel/battery sizes. This includes the constraint that batteries are fully charged at the beginning of their operation, i.e., Equation (17). Note that if the battery is chosen too large, one is paying for unused energy capacity, and if the panel is chosen too large, one is paying for solar energy production but with no place to store the energy. The optimum cost solution for PBG therefore involves adjusting the panel and battery purchases so that an optimum is obtained.

B. Battery/Grid (BG) Configuration

In a BG configuration, electricity from the power grid can be purchased and stored for future use. This may be advantageous when power grid costs are time dependent, e.g., when $c_g(k)$ is not the same for all k. During off-peak hours, when power grid pricing is reduced, battery storage for future use may lead to reduced OPEX costs. By setting $\mathcal{P} = 0$ in LP–PBG we can obtain the offline lower cost bound for the battery/grid case.

C. Solar Panel/Grid (PG) Configuration

In the panel/grid configuration, the capability of storing electricity in off-hours is eliminated, and all the input energy from the solar panels is applied directly to the load whenever possible. Since energy pricing is normally more expensive during daytime hours, there is a good correlation between solar energy availability and higher energy pricing. To formulate the panel/grid problem, LP–PBG can be modified as follows.

$$\begin{aligned}
&\underset{\mathcal{P},\,\epsilon_g(k)}{\text{minimize}} && c_p\ \mathcal{P} + \sum_{k\in\mathcal{K}} c_g(k)\ \epsilon_g(k) && && \text{(LP–PG)}\\
&\text{subject to} && \mathcal{L}(k) \le \mathcal{P}\ \zeta\ \mathcal{S}(k) + \epsilon_g(k) && \forall k \in \mathcal{K} && (20)\\
&&& 0 \le \epsilon_g(k) && \forall k \in \mathcal{K} && (21)\\
&&& 0 \le \mathcal{P} && && (22)
\end{aligned}$$

In this case the LP selects the best solar panel size and power grid energy purchases. This is subject to providing sufficient load energy during each time epoch.

D. Energy Revenue (ER) Configuration

The ER configuration is a modification to PBG where unused energy may be returned to the power grid. This type of situation is currently available in various countries. In Canada, for example, the purchase price that utilities offer for excess energy is about four times that which they sell to their customers [9]. In this case we define $\epsilon_r(k)$ to be the energy sold to the power grid during time epoch k. The objective function in LP–PBG will now become

$$c_c + c_b\ \mathcal{B}_{max} + c_p\ \mathcal{P} + \sum_{k\in\mathcal{K}} c_g(k)\ \epsilon_g(k) - \sum_{k\in\mathcal{K}} r_g(k)\ \epsilon_r(k) \quad (23)$$

where $r_g(k)$ is the unit price *paid* by the power grid for surplus energy at time k. We also introduce two new optimization variables, $\epsilon_{bg}(k)$ and $\epsilon_{sg}(k)$, which are battery-to-grid and solar-to-grid energy transfers during time interval k. Inequality (9) now becomes

$$\mathcal{B}(k) \le \mathcal{B}(k-1) + \eta_b^+(\epsilon_{sb}(k) + \epsilon_{gb}(k)) - \epsilon_{bl}(k) - \epsilon_{bg}(k) \quad (24)$$

for all $k \in \mathcal{K}$, and expressions (11) and (13) will change to

$$\epsilon_{sb}(k) + \epsilon_{sl}(k) + \epsilon_{sg}(k) \le \epsilon_s(k) \quad \forall k \in \mathcal{K} \quad (25)$$

and

$$\epsilon_{bl}(k) + \epsilon_{bg}(k) \le \mathcal{B}(k-1) \quad \forall k \in \mathcal{K} \quad (26)$$

We must also have that

$$\epsilon_r(k) \le \epsilon_{sg}(k) + \eta_b^-\ \epsilon_{bg}(k) \quad \forall k \in \mathcal{K} \quad (27)$$

The LPs formulated above have access to all input data at once and therefore they provide only lower bounds on cost. However, these formulations can be used as an excellent basis for the offline design of the solar power add-on, which is the approach taken. When the solar add-on is deployed however,

Algorithm 1 Grid Purchase Last (GPL) Algorithm

1: **for all** $k \in [1, 2, \cdots, \infty)$ **do**
2: **if** $\mathcal{L}(k) \leq \epsilon_s(k)$ **then**
3: Supply load, $\mathcal{L}(k)$, using solar energy and place any residual energy in the battery, i.e., $\epsilon_{sb}(k) = \epsilon_s(k) - \mathcal{L}(k)$.
4: **else if** $\epsilon_s(k) < \mathcal{L}(k) \leq \epsilon_s(k) + \eta_b^- \mathcal{B}(k-1)$ **then**
5: Supply $\mathcal{L}(k)$ using both solar and battery energy, i.e., $\epsilon_{bl}(k) = \epsilon_s(k) - \mathcal{L}(k)$.
6: **else**
7: Supply $\mathcal{L}(k)$ using available solar and battery energy plus a grid power purchase, i.e., $\epsilon_{gl}(k) = \epsilon_s(k) + \eta_b^- \mathcal{B}(k-1) - \mathcal{L}(k)$.
8: **end if**
9: **end for**

online energy scheduling algorithms are needed which control real-time energy flow, purchases and storage decisions. In the following section, three online algorithms are proposed and performance results are compared in Section V.

IV. On-Line Energy Scheduling Algorithms

The objective of the online algorithms is to schedule real-time energy use with minimum OPEX cost. We first consider the PBG configuration discussed in Section III-A. The algorithms to be discussed are also applicable for the BG and ER configurations.

A. Grid Purchase Last (GPL) Algorithm

The Grid Purchase Last (GPL) algorithm is motivated by the fact that if grid energy pricing is fixed, $c_g(k) = c_g$ for all k, then a feasible minimum cost solution for LP–PBG can always be obtained when $\epsilon_{gb}(k) = 0$ for all k, i.e., in order to achieve the optimum offline bound, it is never necessary to store power grid energy in the battery. This result is proven in a report which is available upon request from the authors. Accordingly, the GPL algorithm defers any power grid purchases as long as possible. The details are shown in Algorithm 1 and described as follows. In Step 2, if there is sufficient solar energy to power the load, this is the option taken. In this case any residual solar energy, $\epsilon_s(k) - \mathcal{L}(k)$, is made available for storage in the battery. If there is insufficient solar energy, then energy is also drawn from the battery to make up the shortfall, as shown in Step 5. Finally, only if solar and battery reserves are insufficient is energy purchased from the power grid (Step 7). The GPL algorithm is very simple and is likely to be the sort of default used in many practical situations. However, there are many scenarios where its performance is not very good. In the following, two other algorithms are introduced which take into account solar insolation factors, traffic loading and grid energy pricing.

B. Solar Load Optimization (SLO) Algorithm

The SLO Algorithm uses predictions of input solar insolation values, $\mathcal{S}(k)$, over a future window of duration $w\Delta t$ as a basis for its energy scheduling decisions. The predictions that we use are based on the algorithm first proposed in [10]. This is used to predict both future solar energy, $\mathcal{S}(k)$ and the load, $\mathcal{L}(k)$. Note that predicting the granular details of long term solar availability is known to be very difficult. However, this level of detail is not needed in our case, mainly due to the averaging effects of the battery, and as a result what is important is that we have reasonable averaged predictions. Using these *predicted* values, the algorithm solves a linear program over the next w discrete time epochs, which gives estimated values of $\epsilon_g(k)$ to use for power grid energy purchases. More formally, at time k the algorithm estimates the values of $\mathcal{S}(i)$ and $\mathcal{L}(i)$ for $i = k+1, k+2, \ldots, k+w$, and uses these estimates with the known value of $\mathcal{B}(k)$ in LP–PBG to determine the estimated future values of $\epsilon_g(j), \epsilon_{gb}(j), \epsilon_{gl}(j), \epsilon_{sb}(j), \epsilon_{sl}(j)$, for $k \leq j \leq k+w$. Note however, that the objective function in LP–PBG is replaced by

$$\sum_{i=k}^{i+w} \epsilon_g(i)\, c_g(i) \tag{28}$$

since the battery and panel sizes are already determined. The remaining variables give the amount of power grid energy that should be purchased in each future time epoch. The above result gives estimates for the variables indicated, however, the "next step" values for $k+1$ are the only ones used. The LP solution gives a set of grid energy variables, $\epsilon_g(j)$ for $j = k, k+1, \ldots, k+w$, that should be purchased over this time period. Since the algorithm is run every Δt, only the result for the current time period, k, is purchased.

Algorithm 2 Solar Load Optimization (SLO) Algorithm

1: **for all** $k \in [1, 2, \cdots, \infty)$ **do**
2: Use the prediction algorithm from Reference [10] for $k+1 \leq i \leq k+w$ with the updated objective (28) to find the target variables including $\epsilon_g(i)$ for $i = k, k+1, \ldots, k+w$.
3: Implement the energy flow in accordance with the solution obtained in Step 2. If $\mathcal{L}(k)$ is higher than its prediction, or if $\mathcal{S}(k)$ is lower, then draw the additional energy needed from the battery, i.e., increase $\epsilon_{bl}(k)$ above its predicted value. If this is insufficient, purchase additional energy from the power grid, i.e., increase $\epsilon_{gl}(k)$ to make up the shortfall.
4: **end for**

C. Solar Load Simulation (SLS) Algorithm

Instead of solving an LP at each time epoch, when a grid energy purchase is needed, the SLS Algorithm may purchase the energy early, provided that there is room in the battery and the purchase price is lower. As in SLO, predicted values for solar insolation and load are used for a window of w time epochs extending into the future. In Step 3 of Algorithm 3, the predicted values in Step 2 are used to find the battery energy levels at each time epoch over next w intervals. This is accomplished by simulating the battery energy recursion (1), subject to Equations (2) to (6) using the GPL Algorithm. We then find the first time period, p, where a future power grid energy purchase is predicted, i.e., Step 4. If the current energy purchase price (at time k) is less than all other time periods between k and p, and purchasing energy would not overflow of the battery for $i \in \{k+1, \ldots, p\}$, then we move the grid energy purchase from time p to k. This is shown in Steps 5 and 6, i.e., when grid energy is required the algorithm looks for a time period between the current time k and time p which has the lowest energy price. If the energy price at the current time period is less over all other time periods from k to p, the

Algorithm 3 Solar Load Simulation (SLS) Algorithm

1: **for all** $k \in [1, 2, \cdots, \infty)$ **do**
2: Obtain the predictions using Reference [10] for $i \in \{k+1, k+2, \ldots, k+w\}$.
3: Using the predicted values from Step 2, and known values of available solar energy and battery energy level at time k, simulate the system over $\{k, \ldots, k+w\}$ using the battery energy recursion (1), and (2) to (6). When doing this, use the GPL Algorithm.
4: Find $p = \min j : 0 < \epsilon_g(j)$ for all $j \in \{k+1, \ldots, k+w\}$.
5: **if** $c_g(k) < c_g(i)$ **AND** $\mathcal{B}(i) < \mathcal{B}_{max}$ for all $i \in \{k+1, \ldots, p\}$ **then**
6: $\epsilon_g(k) := \epsilon_g(k) + \min(\epsilon_g(p), \mathcal{B}_{max} - \mathcal{B}(k))$.
7: **end if**
8: **end for**

required energy is purchased, otherwise the algorithm waits. The variables used in the recursion are then updated.

V. Simulation Results

The methodology used for our experiments is as follows. First, the solar add-on is configured *offline*, using the bounds formulated in Section III. This is done using historical solar insolation traces for the city of Boston MA., for the years spanning 1967-1978. This result determines the CAPEX cost of the solar add-on. The configured system is then operated using the *online* energy scheduling algorithms proposed in Section IV. This is done using solar insolation traces and node energy loading which are *different* from those which are used in the offline design phase. For the online experiments we use solar insolation data from the years 1979-1990 for the same geographic location. In the presented results, some of the graphs include separate "Bound" curves. These are obtained by evaluating the appropriate LP optimization from Section III *using the exact online input data*. Since this data is provided all at once to the optimization, it gives a true lower bound on the cost for a given online experiment. These bounds are useful for comparisons, however, they are clearly not realizable by a causal online algorithm. In our experiments we use a model obtained from the observations in [11] that show a 24 hour sinusoidal periodicity in averaged basestation power consumption. Accordingly, we define the average power usage of the load by P_L. In addition, the minimum and maximum value of energy consumption of the node occurs at 5 a.m. and 5 p.m., respectively. Based on the results presented in [12] which show a time-correlated daily periodicity in energy use, we adopt the following node power consumption model where $P(k)$ is the power consumption at the start of time epoch k

$$P(k) = P_L(1 + \frac{1}{3}\cos(\frac{\pi}{12}(k\Delta t + 7))) + \gamma_n \quad \forall k \in \mathcal{K} \quad (29)$$

where γ_n is a normally distributed random variable with a mean of zero and a standard deviation of 70W, which is used to model random perturbations in the loading. Note that in Equation (29), $k = 0$ corresponds to midnight at the start of the first day considered in $\mathcal{T}$. The actual node energy requirements are therefore given by $\mathcal{L}(k) = P(k)\,\Delta t$.

A *Time of Use* pricing model is used which has two modes. It is assumed that electricity pricing is on-peak from 7 a.m. to 6 p.m., and the price during these hours is 1.5 times the average, and the off-peak pricing is half the average [13]. Unless otherwise stated, the unit battery and panel specifications as well as other parameter values are given in Table II. The default value for P_L is set to 1450 W [14].

Batteries	
Capacity	150 Ah
η_b^+, η_b^-	0.92
Cost	\$229 CAN

Solar Panels	
Size	$1.65 \times .992$ m^2
ζ	0.1497
Cost	\$197 CAN

TABLE II
Default Parameter Settings

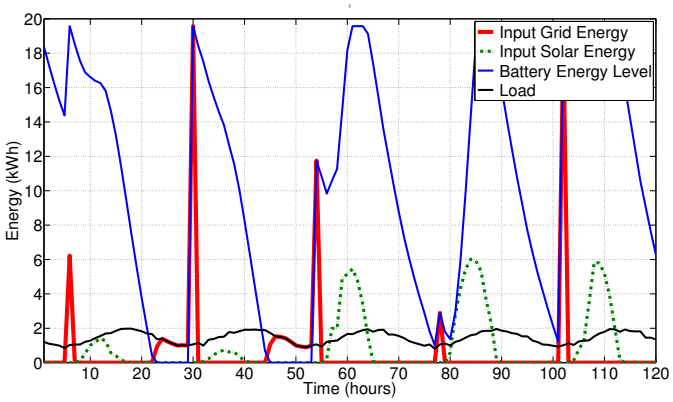

Fig. 2. Energy Flow Time Line Example.

A. Solar Panel, Battery and Grid (PBG) Case

An example is first shown which illustrates energy flow in the node. Figure 2 shows the evolution of the energy components for a five day period starting at the first day of January. It can be seen that the first two days provide only small levels of solar energy input and this leads to significant grid power purchases in days 2 and 3. This is shown by the high vertical spikes. The daily solar input increases significantly at that point and only small grid power purchases are needed in the last two days. As would be expected, these occur in the hours just before sunrise as the battery level bottoms out.

In the second set of results, the performance of the PBG configuration is compared with the cases where we operate the system with grid-only (GO) powering and solar-only (SO) powering. The GO case is the original system without any addition, and the second is with a solar/battery add-on which is provisioned to be energy sustainable, i.e., no grid purchases are needed. Results are evaluated for deployment time periods ranging from 2 to 12 years. The average energy price varies over a wide range from 0.1 to 0.5 $\$/kWh$. In the first of these results shown in Figure 3, the average energy price is set to 0.3 \$/kWh, with the daily fluctuation discussed above, and the performance of the algorithms in terms of the total cost, i.e., the sum of CAPEX and OPEX costs, is compared for an add-on deployment time from 2 to 12 years. An interesting result is that by properly combining the two configurations, we can obtain a system with significantly less total cost. From Figure 3, the GO scenario is up to about 100% more expensive than the PBG configuration even when the Grid Purchase Last (GPL) algorithm is used. However, the GPL

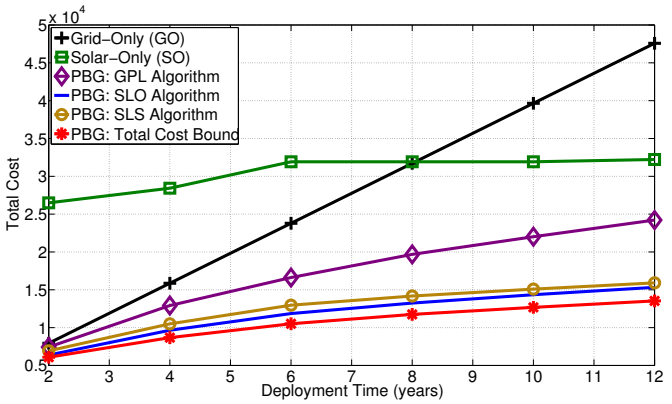

Fig. 3. Example Comparison of GO, SO and PBG Configurations.

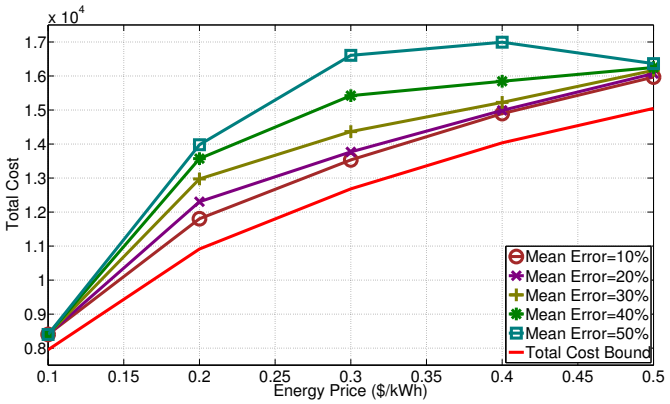

Fig. 4. Total Cost with Load Error Prediction.

scheduler has relatively poor performance compared with SLO and SLS. This is because it does not take into account the daily grid power pricing differences. In this case, where we have used practical numbers, the cost of the system using GO is about 210% higher than that obtained with the SLO and SLS algorithms. In results that we have not shown, we find that when the grid pricing is fixed, i.e., $c_g(k) = c_g$ for all k, the GPL scheduler performance is about the same as SLO and SLS.

The proposed models can also be used to assess the physical requirements of a proposed deployment scenario. For example, in these results, the numbers of solar panels vary widely. At .2$/kWh pricing and a two year time period, a 3×3 standard panel arrangement is needed. When energy pricing increases to .5$/kWh and a 10 year time period, a 6×6 panel arrangement is required.

Results have also been obtained which explore the effects of errors in load prediction. This was done in two different ways. In the first we assumed that there are random (Gaussian) errors in our hourly predictions but that our average power consumption is known. This would be correspond to the case where cyclic trends in power consumption are predictable from one day to the next as is often the case. We found that the cost results were very insensitive to this type of error even for a very large error variance. The reason for this is that the panel/battery heavily integrates the energy demands, effectively averaging/smoothing out this type of error. However, results were also obtained when the mean loading is unknown. Figure 4 shows the total cost versus energy price with different mean errors. These results include random Gaussian errors with a standard deviation of 70W. The figure shows that as the mean error increases, i.e., the ratio of the mean of the estimated load to the mean of the actual load, the costs may also increase. Interestingly, the curves converge at both low and high values of energy cost. This happens because when energy pricing is low, operating costs are dominated by power grid purchases, but since the price is low, costs eventually drop. Conversely, when energy pricing is high, the system increasingly resorts to solar energy and hence energy pricing drops again. At these two extremes, the system is dominated by either power grid or solar energy input, and therefore the results are less sensitive to the quality of the energy management algorithm. In the region between these two extremes however, it can be seen that higher errors may occur compared with the case where node loading is known. In the example shown in Figure 4 the worse error is about 20% when the mean error is 50%, which seems reasonable.

B. Solar Panel/Grid (PG) Configuration

Using a PG configuration is an interesting option since daytime solar energy output correlates well with the times when node energy consumption and grid energy pricing tends to be higher. In these experiments, LP–PG has been used to determine the optimum cost for variable energy pricing and for different deployment periods.

The total cost bound for PG along with its online results in comparison with the Grid-Only case are shown in Figure 5. It can be seen that there is very little difference between the bound and the online results. This is because there is no intelligent energy scheduling required, i.e., any available solar energy is immediately used, and the power grid fills in any shortfall. Similarly, if the solar energy is higher than that needed, the surplus is lost.

Results have also been obtained which show the fractional split between total cost and energy usage for the PG configuration. For the system parameters used above, we find that the contribution to total energy provided by solar power is about 16%, which is not insignificant. The contribution to total cost is about 24%, but decreases slightly with deployment time amortization, as would be expected. The intuition that the PG configuration is able to provide significant amounts of energy during daytime hours is correct.

C. Battery/Grid (BG) Configuration

The converse case to PG is to use a battery only, i.e., BG, node add-on. In this case all consumed energy will be that from the power grid. This configuration makes no sense if energy pricing is fixed, i.e., when $c_g(k) = c_g$ for all k, and therefore it is somewhat limited in its overall usefulness. However, when there are temporal energy cost differences, this can be exploited by storing energy and by shifting energy purchases to times when the energy costs are lower. This makes sense since, in practice, elevated pricing tends to occur over long time periods during peak usage hours.

Figure 6 shows a comparison of total cost versus deployment time amortization for the BG and PBG configurations.

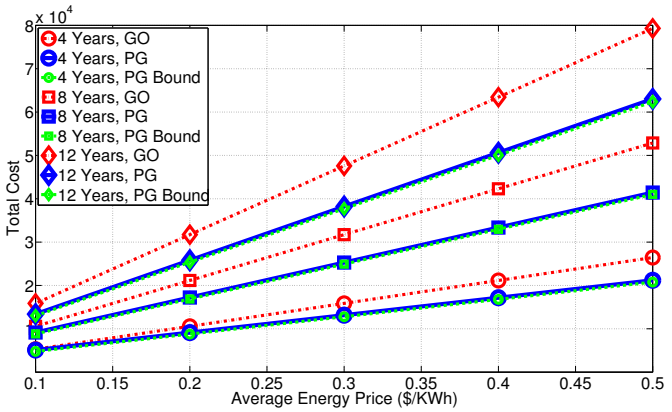

Fig. 5. Total Cost (OPEX and CAPEX) for a Panel/Grid (PG) Configuration Compared with the Grid Only (GO) case.

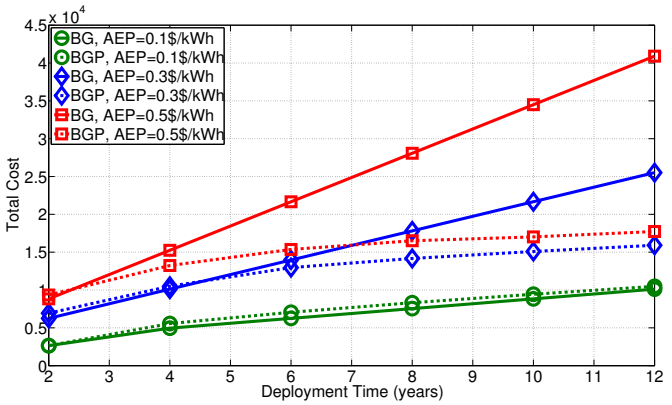

Fig. 6. Total cost (OPEX and CAPEX) for the Battery/Grid (BG) Configuration Compared to PBG Case.

Different curves are shown for different Average Energy Pricing (AEP) energy pricing. At the left of the graph, the results show that for short deployment times there is little cost advantage in providing the system with solar panels. The reason for this is that solar panels are expensive and their cost cannot be recouped over these short time periods. The same is true for very low energy pricing. In this case (the lower curves in Figure 6), expenditure is focused on grid energy purchases, so again, the system is best to avoid solar energy use. However, it can be seen that for more typical energy costs and amortization periods, there is a significant advantage in including solar energy. At the right of the graph, the BG cost is over double that of PBG. This improvement over the BG case is due to the fact that the "energy time shifting" can occur over large time periods and is not subject to the energy loss associated with the PG configuration's inability to store energy. Clearly, for the parameters that we are considering, BG provides better cost saving performance than PG. This scenario could change if, for example, the relative unit costs of the battery and solar panel were to dramatically change from their current values.

D. Energy Revenue (ER) Configuration

In this section it is assumed that the node add-on is configured to sell unused energy back to the power grid. The LP introduced in Section III-D is used to determine the

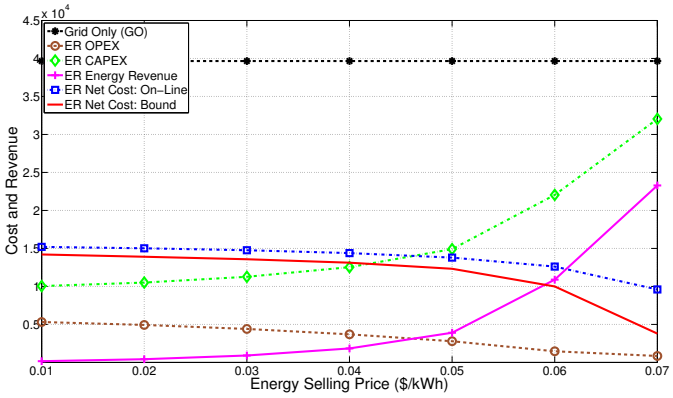

Fig. 7. Energy Revenue Example with PBG Configuration

CAPEX and provisioning costs using the modified version of LP–PBG as discussed in that section. The online algorithm therefore schedules grid energy purchases, but also determines if surplus energy should be sold back to the grid at each time epoch.

Simulation results when the average energy price for purchasing electricity differs from the selling price are shown in Figure 7. The average energy purchase price is 0.3 $/kWh, the add-on amortization time is set to 10 years, and $c_c = \$300$ which was taken from Reference [15]. It is clear from this figure that permitting energy revenue strongly affects the economics of the node add-on. In this figure, separate curves have been shown for the add-on CAPEX and selling profit values. With a revenue capability, the overall cost is seen to decrease as the energy selling price increases. It can be seen that if the selling price increases, the optimizer aggressively increases CAPEX expenditures.

E. Geographic Location

A wide variety of results have been obtained for other geographic locations, including New York, Atlanta, Phoenix, and Seattle. An example of total cost versus energy pricing for the PBG configuration is shown in Figure 8. In this graph we have used the same parameters as in Section V-A with our best online algorithm, SLO. As expected, we find that the availability of solar energy has a strong impact on the total cost. For example, Seattle has a marine climate with a relatively high fraction of overcast days that significantly increase solar CAPEX costs. Atlanta has a temperate climate, and Phoenix has a subtropical arid climate with a year-round abundance of solar energy. It can be seen that Boston and New York give very similar results. When comparing Phoenix to Seattle there is about a factor of two cost difference at the high energy price point shown. Note that the total cost differences decrease with energy pricing (to a ratio of about 1:1.3) since this leads to a reduction in solar capital expenditures. Clearly there would be no use for solar power in the limit as power grid energy become free, and obviously the economics of a solar add-on are highly location dependent.

Using the same system assumptions, the differences in location have been considered from a total energy usage viewpoint. At the one extreme for Phoenix, solar energy supplies about 92% of the energy needs. At the other extreme,

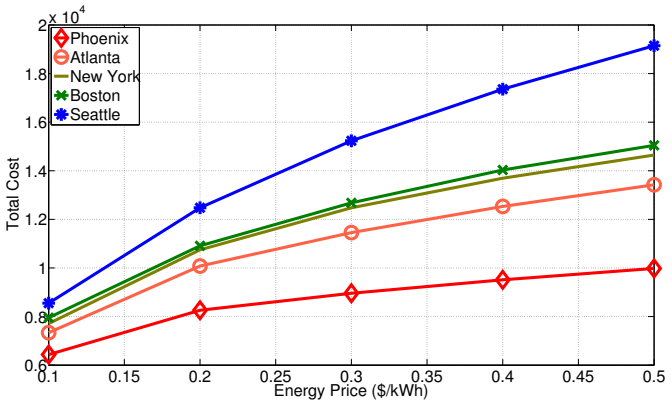

Fig. 8. Total Cost (OPEX and CAPEX) for Different Locations (SLO Algorithm).

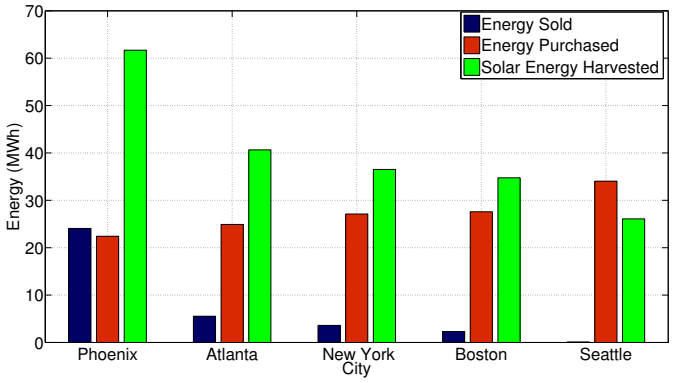

Fig. 9. Energy Use for Different Locations (SLO Algorithm).

for Seattle, we find that power grid energy is providing almost 40% of its energy requirements. The solar energy fractions for Atlanta, New York City and Boston, are about 20%, 22% and 24%, respectively. This trend of course, is expected due to the decrease in solar energy availability.

Figure 9 shows an example using the same assumptions as in Section V-D which illustrates the differences in energy use in the revenue configuration for the different geographic locations. The cities appear in decreasing order of energy sold to the power grid. The graph shows that there are significant differences in energy use. In more solar rich locations such as Phoenix, there is much more opportunity for selling energy than in more temperate locations. For example, we see that there is about a factor of ten difference between solar energy sold in Phoenix compared with Boston. At the same time, in locations where solar insolation is more highly variable, such as in Seattle, the system must rely more on fulfilling its energy needs with power grid purchases.

VI. Conclusions

In this paper, we have considered the operating and capital costs of providing a solar powered add-on to power grid operated communications infrastructure nodes. Online energy scheduling algorithms were also introduced. Lower bounds on the costs were also derived using linear programming (LP) formulations, where solar components are sized using solar insolation and projected loading data.

To compare the performance of the proposed algorithms, solar insolation traces for the city of Boston, MA. were used. Simulation results show that when comparing with the grid energy only case, using the proposed energy management scheduling algorithms results in a 40% to 78% reduction in the total cost. This is achieved when a combination of batteries and panels are used to supplement purchased power grid energy. The improvements obtained are 21% and 48% for the panel/grid and battery/grid configuration cases, respectively. Simulation results were also performed for other cities with different solar insolation profiles. Results show that the algorithms achieve better cost improvements when solar power is more plentiful.

References

[1] H. A. M. Maghraby, M. H. Shwehdi, and G. Al-Bassam, "Probabilistic Assessment of Photovoltaic (PV) Generation Systems," *IEEE Transactions on Power Systems*, vol. 17, no. 1, pp. 205–208, 2002.

[2] M. Gruber, O. Blume, D. Ferling, D. Zeller, M. Imran, and E. Strinati, "EARTH: Energy Aware Radio and Network Technologies," in *20th IEEE International Symposium on Personal, Indoor and Mobile Radio Communications*, 2009.

[3] S. Chowdhury and S. Aziz, "Solar-Diesel Hybrid Energy Model for Base Transceiver Station (BTS) of Mobile Phone Operators," in *2nd International Conference on the Developments in Renewable Energy Technology (ICDRET)*, 2012.

[4] W. Yu and X. Qian, "Design of 3kW Wind and Solar Hybrid Independent Power Supply System for 3G Base Station," in *Second International Symposium on Knowledge Acquisition and Modeling, KAM'09*, vol. 3, 2009, pp. 289–292.

[5] P. Nema, S. Rangnekar, and R. Nema, "Pre-feasibility Study Of PV-Solar/Wind Hybrid Energy System for GSM Type Mobile Telephony Base Station in Central India," in *The 2nd International Conference on Computer and Automation Engineering (ICCAE)*, vol. 5, 2010, pp. 152–156.

[6] T. Han and N. Ansari, "ICE: Intelligent Cell BrEathing to Optimize the Utilization of Green Energy," *IEEE Communications Letters*, vol. 16, no. 6, pp. 866–869, 2012.

[7] Z. Zheng, S. He, L. Cai, and X. Shen, "Constrained Green Base Station Deployment with Resource Allocation in Wireless Networks," *Handbook on Green Information and Communication Systems, John Wiley & Sons, Inc.*, 2012.

[8] U.S. Department of Energy, "National Solar Radiation Database (NSRDB)," Renewable Resource Data Center (RReDC), National Renewable Energy Laboratory (NREL), 2012. [Online]. Available: http://www.nrel.gov/rredc/

[9] Ontario Power Authority, "http://fit.powerauthority.on.ca/," 2013. [Online]. Available: http://fit.powerauthority.on.ca/

[10] M. Ali, B. Al-Hashimi, J. Recas, and D. Atienza, "Evaluation and Design Exploration of Solar Harvested-Energy Prediction Algorithm," in *Design, Automation & Test in Europe Conference & Exhibition (DATE)*, 2010, pp. 142–147.

[11] L. Correia, D. Zeller, O. Blume, D. Ferling, Y. Jading, I. Godor, G. Auer, and L. Van Der Perre, "Challenges and Enabling Technologies for Energy Aware Mobile Radio Networks," *IEEE Communications Magazine*, vol. 48, no. 11, pp. 66–72, 2010.

[12] P. Frenger, P. Moberg, J. Malmodin, Y. Jading, and I. Gódor, "Reducing Energy Consumption in LTE with Cell DTX," in *73rd IEEE Vehicular Technology Conference (VTC Spring)*, 2011.

[13] Y. Peng, G. Tang, and A. Nehorai, "A Game-Theoretic Approach for Optimal Time-of-Use Electricity Pricing," *To be Published in IEEE Transactions on Power Systems*, no. 99, 2012.

[14] O. Arnold, F. Richter, G. Fettweis, and O. Blume, "Power Consumption Modeling of Different Base Station Types in Heterogeneous Cellular Networks," in *Future Network and Mobile Summit*, 2010.

[15] SunForce Inc., "http://www.sunforceproducts.com/," 2013. [Online]. Available: http://www.sunforceproducts.com/